Field and flow perturbations in the October 18-19, 1995, magnetic cloud

L. Janoo,[1] C. J. Farrugia,[1] R. B. Torbert,[1] J. M. Quinn,[1] A. Szabo,[2] R. P. Lepping,[2] K. W. Ogilvie,[2] R. P. Lin,[3] D. Larson,[3] J. D. Scudder,[4] V. A. Osherovich,[5] and J. T. Steinberg[6]

Abstract. We examine magnetic field and plasma perturbations in the October 18-19, 1995, magnetic cloud. Besides the front boundary, the 3-s-averaged magnetic field measurements made by the Magnetic Field Investigation on the Global Geospace Mission spacecraft Wind reveal a further 15 clear magnetic field directional discontinuities (DDs) with field rotations $>15°$, each lasting for $\sim$1 min. A number of these DDs are clustered near the trailing edge of the cloud. Using 3-s resolution proton data from the Three-Dimensional Plasma and Energetic Particle Experiment on Wind, we find that these DDs are accompanied by perturbations in the flow. We find that except for the front boundary, which is a clear tangential discontinuity, all the others are rotational. Across the DDs the bulk flow speed is sometimes enhanced and sometimes depressed. Changes in proton temperature across the DDs suggest a more elaborate structure, for example, a reconnection layer. In a search for large-scale regularities, we apply minimum variance analysis to determine the normals to contiguous 1-hour-long stretches of the cloud data and find that there are large-scale structures ordering the field and the flow for the first 21 hour of cloud data. Thus we identify three coherent segments of several hours' duration each with a well-defined normal, but the normals to the individual segments are very different from each other. In particular, one segment in the cloud $B_z < 0$ phase is almost orthogonal to another segment in the $B_z > 0$ phase. The normals to the DDs within a given segment are closely aligned with the normal to that segment. For the last 6 hours of cloud data, no coherent structure was found since no reliable normals could be determined. Studying flow anisotropies of electrons in the energy range 0.1 - 100 keV and changes in intensity in the >1 keV electrons, *Larson et al.* [1997] inferred several instances of disconnection of cloud field lines from the Sun, which were attributed to reconnection between adjacent bundles of cloud field lines. Our results are supportive of this interpretation. Furthermore, our results suggest the presence of detailed substructure in, and/or large distortions of, the magnetic cloud which reached 1 AU on October 18-19, 1995.

[1]Institute for the Study of Earth, Oceans, and Space, University of New Hampshire, Durham.

[2]NASA Goddard Space Flight Center, Code 692, Greenbelt, Maryland.

[3]Space Sciences Laboratory, University of California, Berkeley, California.

[4]Department of Physics and Astronomy, University of Iowa, Iowa City.

[5]NASA Goddard Space Flight Center, Hughes STX, Greenbelt, Maryland.

[6]Center for Space Research, Massachusetts Institute of Technology, Cambridge.

1. Introduction

Larson et al. [1997] have recently pointed out some interesting features of the magnetic cloud observed by the Wind spacecraft which passed Earth on October 18-19, 1995. Using energetic electron data in the $1 - 10^2$ keV energy range from the Three-Dimensional Plasma and Energetic Particle Experiment on Wind, which are produced by the Sun, for example, in solar flares, they were able to show directly the connection of the cloud field lines to the Sun. However, this connection is not maintained throughout the whole duration of cloud passage: an investigation of dropouts in heat flux electrons (in the energy range $\sim$0.1-1 keV) as well as higher-energy electrons indicate that on several occasions, the

connection to the Sun was severed. *Larson et al.* [1997] argue in favor of reconnection of bundles of adjacent field lines as the cause of these disconnections, and they conjecture that they took place many hours before the dropouts were observed at Wind. On occasion, bidirectional streaming of heat flux electrons was replaced by unidirectional flows. They thus ascribed various topologies to the field lines making up the bent flux rope model of these ejecta originally proposed by *Burlaga et al.* [1990]: some lines are connected at both ends to the Sun, some are connected at one end, and some are disconnected.

The field line topology of this magnetic cloud is sufficiently important to warrant an independent investigation. This is the purpose of this paper. We examine primarily magnetic field data and take as our starting point the observation of a number of discontinuities in the cloud's magnetic field. The discontinuities are defined by (1) their brief duration and (2) the large field rotation, where the latter is defined somewhat intuitively by comparing it with the rotation expected in a smoothly spiraling field over a comparable time span. We find that except for the front cloud boundary, the other discontinuities are rotational, a conclusion which supports the reconnection interpretation gained from the electron observations.

The interplanetary profile of the October 1995 magnetic cloud has further intriguing and puzzling features, to which attention has been drawn by, for example, *Burlaga et al.* [1996] and *Lepping et al.* [1997]. Chief among these are (1) the "boxcar" B profile and (2) the flat V profile. As pointed out by *Burlaga et al.* [1996] and *Lepping et al.* [1997], the rear fields are enhanced because of compression by the faster corotating stream overtaking the cloud. The strong fields near the leading edge result from a peculiarly sharp onset and are a feature rarely encountered in magnetic cloud profiles. In previous work, *Farrugia et al.* [1992, 1993] and *Osherovich et al.* [1993] explained asymmetric B profiles with the peak field shifted toward the front side as a result of self-similar expansion. However, the V profile of the October cloud is flat, giving no indication of expansion. Indeed, *Burlaga et al.* [1996] point to the need of studying this profile further.

In the second part of the paper, we make a preliminary attempt at discussing the large-scale structure of this cloud. Since there is no evidence of expansion, we assume a static configuration and use minimum variance analysis to follow the variation of the minimum variance direction as Wind progresses through the cloud. A simple procedure then suggests that there are multiple structures within the cloud. The diverse orientations in space of the individual structures, as obtained from minimum variance, are not readily incorporated into a single coherent structure, unless they result from large-scale distortions. One interpretation is that these substructures arise because of the sporadic reconnection taking place within the cloud. Another, perhaps complementary, interpretation is that they reflect a gross distortion of the flux rope, in part because the cloud is running into much denser material ahead of it and in part because it is being overtaken by a faster stream at its rear. We feel that the analysis outlined here might be useful to the further investigation of the topology of this, and possibly other, magnetic clouds observed by Wind. A proper appreciation of the topology at 1 AU can help in current discussions on the solar origin of this important class of transients.

2. Wind Observations

2.1. Overview: Magnetic Field and Plasma

The Wind spacecraft, launched on November 1, 1994, is one of two NASA spacecraft (the other being the Polar spacecraft) in the Global Geospace Science Initiative, forming part of the International Solar Terrestrial Physics Program (ISTP). The ISTP, which includes many other spacecraft and ground-based facilities, has as focus the investigation of solar and interplanetary phenomena and their effects on the Earth's magnetosphere. Among the scientific objectives of the Wind mission are to (1) provide interplanetary plasma and energetic particle and magnetic field measurements in support of magnetospheric studies and (2) investigate basic plasma processes in the solar wind close to Earth [see *Acuna et al.*, 1995]. In this paper we shall use data from three instruments on Wind: the Magnetic Field Investigation (MFI [*Lepping et al.*, 1995]); the Solar Wind Experiment (SWE [*Ogilvie et al.*, 1995]); and the Three-Dimensional Plasma and Energetic Particle Investigation [*Lin et al.*, 1995]. The reader is referred to these various works for a description of the respective instruments.

Figure 1 shows magnetic field data at 3-s resolution from the MFI. The time interval shown is from 1800 UT, October 18 to 2400 UT, October 19, 1995. Wind was at (175, -4, -13) R_E, and at (176, -2, 13) R_E (GSE coordinates) at 1800 UT, October 18, and 2300 UT, October 19, 1995, respectively. The x axis in Figure 1 is labeled in hours after 0000 UT, October 18. The various panels show from top to bottom the total field (nanoteslas), and the B_x, B_y, and B_z components of the field in GSE coordinates (nanoteslas). The dotted-dashed vertical guidelines in Figure 1 at 19.1 UT, October 18 and ~2300 UT, October 19 show the cloud boundaries in accordance with the identifications of *Lepping et al.* [1997]. Magnetic clouds are defined by (1) enhanced magnetic field strengths relative to ambient values; (2) a large rotation of the magnetic field vector; and (3) low proton temperatures [*Burlaga et al.*, 1981]. As can be seen in Figures 1 and 2 (below), this definition is satisfied. The determination of cloud boundaries is in general uncertain [see *Burlaga*, 1995]. In this case, the front boundary is unproblematic because at 19.1 UT,
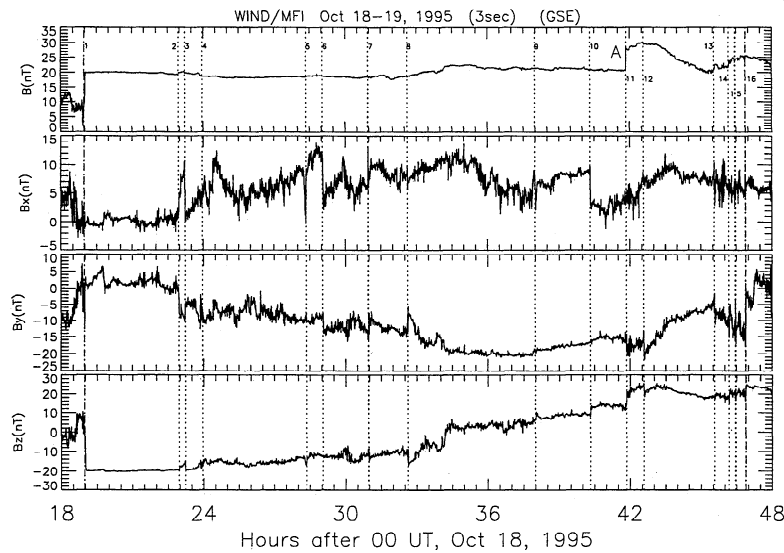
Figure 1. Wind magnetic field data at 3-s resolution for the period 1800 UT, October 18 to 2400 UT, October 19, 1995. The data are plotted in a GSE coordinate system. The magnetic cloud interval is between the dotted-dashed lines. The field directional discontinuities studied in the paper are numbered.

October 18 there is a rapid drop in proton temperature simultaneous with the start of a large rotation of the magnetic field vector. The time at which the rear boundary passes Wind is somewhat uncertain.

The magnetic cloud field executes a large rotation, turning from a due south to a northwest orientation. This large rotation is, however, not smooth as there are manifest fluctuations in all field components. Since the total field is smooth, the field perturbations are orthogonal to the local direction of the field. Among these fluctuations one can make out a number of large discontinuous changes. A smooth field turning $\sim 180°$ in

~ 29 hours would rotate $0.1°$ in ~ 1 min. In Figure 1, we have shown by dotted vertical guidelines the times when the field rotates by an angle larger than $15°$ in ~ 1 min. These are the directional discontinuities (DD) we shall investigate below. There are in all 16 directional discontinuities of this type, as numbered in Figure 1.

Figure 2 shows proton parameters for the same interval as in Figure 1. From top to bottom, the panels show the density (cm^{-3}), bulk flow speed (km s^{-1}), temperature (K), and the GSE V_x, V_y, and V_z components of the flow. The density is from the SWE instrument and has a time resolution of ~ 1.5 min, while the temperature and
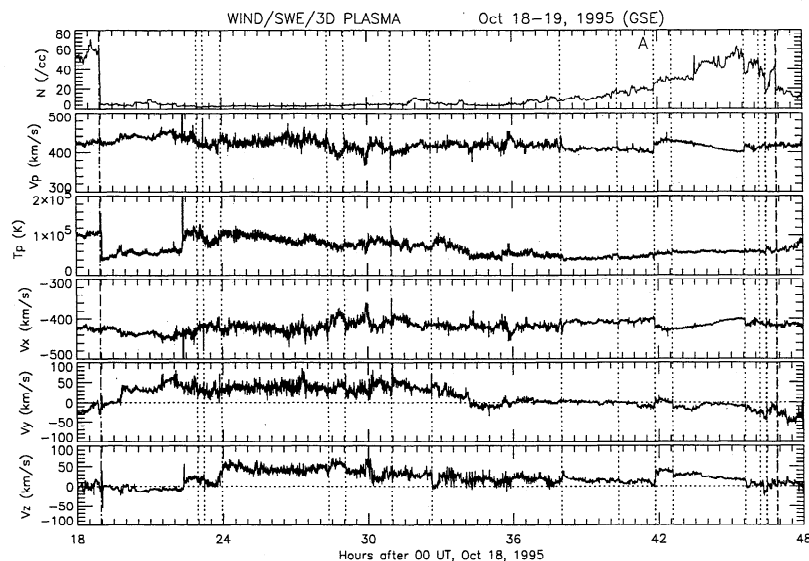

Figure 2. Plasma (proton) observations for the same period as in Figure 1. The vertical lines are drawn at the times of the directional discontinuities shown in Figure 1.

velocity components are from the Three-Dimensional Plasma and Energetic Particle Experiment, and are at 3-s temporal resolution. Ahead of the cloud, the density is high ($\sim$60 cm^{-3}). As argued by *Burlaga et al.* [1998] in connection with another magnetic cloud (that on January 1997), this might be due to the ejecta having been formed within the streamer belt, where densities are typically high. At the front boundary of the magnetic cloud, the density drops from $\sim$60 to $\sim$4 cm^{-3}, a decrease by a factor of 15.. It remains steady around 4 cm^{-3} until hour 31, after which it rises, at first gradually (until hour 36) and then more steeply until hour 45, reaching a peak of 60 cm^{-3} at the rear of the cloud, followed by a decrease to 20 cm^{-3} around hour 47. The temperature drops at the front boundary by a factor of $\sim$2.5 to a value of 4 x 10^4 K, and begins a quasi-linear rise to 6 x 10^4 K up to hour 22.5, where a sudden rise to 10^5 K takes place. From hour 22.5 to hour 36 the temperature profile then decreases linearly to around 4 x 10^4 K. Subsequently, it rises to 6 x 10^4 K at the cloud boundary. Qualitatively, the V_y component is positive till around hour 36; remains around 0 km s^{-1} until hour 41; and then goes negative for the rest of interval in Figure 2. On the other hand, the V_z component starts out with a small negative value till about hour 22.5, and then remains positive for the remainder of the interval. The major flow component, V_x, can be approximated by -425 km s^{-1} for the whole cloud.

In Figure 2, we have drawn in the times of the DDs identified in Figure 1. It can be seen that the large field rotations are often accompanied by impulsive changes in the plasma parameters. However, there are also some cases where impulsive changes in the plasma parameters do not coincide with the DDs we selected for analysis. The DD marked A is a shock-like feature advancing in the cloud from the rear and has been discussed by *Lepping et al.* [1997]. Among the points made by *Lepping et al.* in favour of this interpretation are (1) that it is a thin transition; (2) that consistent estimates of the normal direction to this front are reached by various methods; (3) satisfaction of the MHD jump conditions (except for the temperature); and (4) the observed sense of change of field and plasma parameters, which is consistent with a fast forward shock.

2.2.   Analysis Method

Many people have examined DDs in the solar Wind [see, e.g., *Burlaga*, 1969]. Our analysis is on the DDs in which the field vector rotates by $\geq$15°. Table 1 lists the angle through which the field rotates at the DDs and the average duration. We apply the minimum variance analysis technique of *Sonnerup and Cahill* [1967] and keep only those DDs for which the ratio of intermediate to minimum eigenvalues (λ_2/λ_3) > 2.0, as this guarantees a reliable normal [see *Lepping and Behannon*, 1980]. We apply *Neugebauer et al.*'s [1984] criteria for classifying the DDs, which are as follows:

For a rotational discontinuity (RD)

$$B_n/|\mathbf{B}| \geq 0.4 \qquad [|\mathbf{B}|]/|\mathbf{B}| < 0.2$$

For a tangential discontinuity (TD)

$$B_n/|\mathbf{B}| < 0.4 \qquad [|\mathbf{B}|]/|\mathbf{B}| \geq 0.2 \qquad (1)$$

where $|\mathbf{B}|$ is the larger of the field magnitudes on either side of the discontinuity; B_n is the absolute value of the component of **B** normal to the plane determined by minimum variance; and $[|\mathbf{B}|] = |\mathbf{B_2}| - |\mathbf{B_1}|$ is the difference in absolute values of the fields across the DD. *Neugebauer et al.* [1984] distinguish two other categories, which they term "either" and "neither," but we shall not have occasion to use them here.

We also apply tests based on the plasma data [*Neugebauer et al.*, 1984; *Parks*, 1991]. *Hudson* [1970] shows that in MHD theory rotational discontinuities satisfy the following relationship:

$$[\mathbf{V}] = \pm\sqrt{(\rho A/\mu_0)}[\mathbf{B}/\rho]. \qquad (2)$$

A is the pressure anisotropy of the plasma, defined as

$$A = 1 - \frac{(P_\parallel - P_\perp)\mu_0}{B^2},$$

where $P_\parallel$ and $P_\perp$ are, respectively, the thermal plasma pressures parallel and perpendicular to the magnetic field; μ_0 is the permeability of free space; and $[..]$ denotes the difference between the quantities before and after the discontinuity. For a DD propagating antisunward, the plus sign in (2) is used when the average

Table 1. Field Discontinuities

Number of DDs[a]	Angle Rotated[b]	Average Duration[c]
11	$15 \leq \phi \leq 20$	15 s
2	$20 < \phi \leq 30$	19 s
2	$30 < \phi \leq 40$	45 s
1	$\phi > 40$	3 min

[a]Field directional discontinuities (DDs) in 3-s-resolution of magnetic field data from Wind.
[b]The ϕ is the angle that the field rotates.
[c]Average duration for all the discontinuities in this angular range.

interplanetary magnetic field points towards, and the minus sign when it points away from, the Sun. In the absence of more exact knowledge, we assume the plasma to be isotropic. In the normal solar wind, parameter A is estimated as ~0.9 [*Burlaga*, 1971]. In coronal mass ejections (of which magnetic clouds form a subset) observed by ISEE 3, $T_{\parallel}$ is generally greater than $T_{\perp}$, with a typical ratio $T_{\parallel}/T_{\perp} \sim 2$ [*Gosling et al.* 1987]. Using $T = 1/3(2T_{\perp} + T_{\parallel})$, we obtain $A = 1 - 0.75\beta$, where β is the average proton beta. For the October 1995 magnetic cloud, $\beta < 0.05$ [*Lepping et al.*, 1997] which gives $A \sim 0.96$. Thus the assumption of isotropy seems to be well fulfilled in our case.

Let θ be defined as the angle between $[\mathbf{V}]$ and $[\mathbf{B}/\rho]$. For an RD, θ should ideally be 0 or 180°, while it can take any value for a TD. A further important parameter is the angle α, introduced by *Belcher and Solodnya* [1975] and defined by the following relation:

$$\tan(\alpha) = \frac{\sqrt{\mu/\rho}|[\mathbf{V}]|}{|[\mathbf{B}/\rho]|} = \frac{\sqrt{\mu/\rho}|\mathbf{V}_2 - \mathbf{V}_1|}{|\mathbf{B}_2/\rho_2 - \mathbf{B}_1/\rho_1|} \quad (3)$$

Ideally (i.e., not taking account of observational and other errors), for an RD, the angle α should be close to 45°. For a TD the angle α can take on any value between 0° and 90°.

Besides these field and flow relations, we consider jump conditions on the density and the temperature. For a TD and assuming isotropy, there can be arbitrary jumps in these parameters constrained only by the requirement of total pressure balance. For an RD and assuming isotropy, there are no jumps in either the density or the temperature [*Parks*, 1991].

2.3.   Specific Examples

Before presenting our general results, we discuss three examples of discontinuities inside the magnetic cloud. Figure 3 shows plasma and field data in GSE coordinates for discontinuity D8 (Figure 1). A time interval of 3 min is shown, centered on hour 38.005. The panels show from top to bottom the density, bulk flow speed, temperature and the three, paired components of the velocity and magnetic fields. The horizontal lines indicate intervals before and after each discontinuity, in which we average values to form jumps in physical quantities across the DD. Across the discontinuity, the magnetic field rotates by 15°. Minimum variance analysis on this discontinuity yields a intermediate-to-minimum eigenvalue ratio $(\lambda_2/\lambda_3) = 71.1$. (Table 2), indicating a reliably determined normal to the maximum variance plane. The field component normal to the discontinuity is 21 nT. $B_n/|\mathbf{B}|$ for this discontinuity is 0.99, and $[|\mathbf{B}|]/|\mathbf{B}| = 0.01$. Therefore (1) is satisfied and the discontinuity is rotational. This conclusion is corroborated by a calculation of angles θ (the angle between $[\mathbf{V}]$ and $[\mathbf{B}/\rho]$) and α (equation (3)), which are ~9° and 33°, respectively, i.e., close to the expected values for an RD.
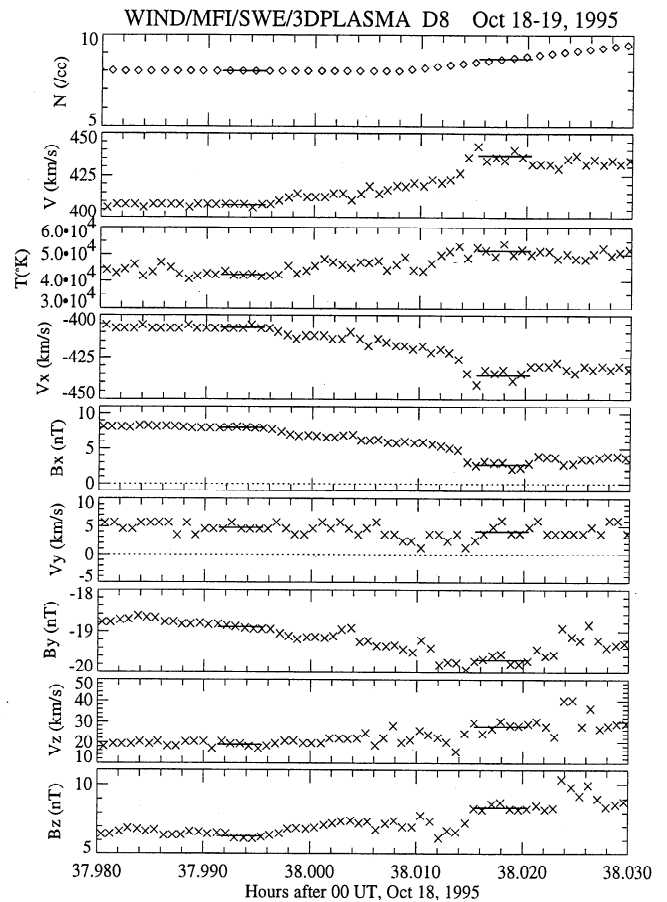

Figure 3. Wind magnetic field and plasma data at 3-s resolution for the discontinuity around 38.005 hours (~14.005 UT, October 19, 1995). The solid lines are the average values before and after the discontinuity. There is a flow speed enhancement and a proton temperature rise at the discontinuity, but the density stays constant.

We note that while across the discontinuity the density at this (low) resolution does not change, there is a ~20% temperature rise and a clear flow enhancement of about 35 km s^{-1}. The rise in temperature is suggestive of more structure than just an RD, for example, a reconnection layer. However, an analysis of this is beyond the scope of this paper.

The second example occurred near the cloud rear at ~42.58 hours (discontinuity D10 in Figure 1). Figure 4 shows 2.4 min of data in the same format as Figure 3. Minimum variance analysis gives an intermediate-to-minimum eigenvalue ratio of 5.5 (Table 2) and a normal field component B_n of 28.4 nT. The field-based test (equation (1)) is satisfied for an RD. The angles θ and α are ~ 3° and 37°, respectively, confirming the RD identification inferred from the minimum variance analysis. As in the previous example, there is again a temperature rise but no bulk speed or density change across this discontinuity.

The third example refers to a discontinuity centered at 30.97 hours (D6 in Figure 1). Figure 5a shows 1.2

Table 2. Discontinuity Field Test

DDs[a]	Time[b]	B_n[c]	$\|\mathbf{B}\|$[d]	$\|[\mathbf{B}]\|$[e]	$\frac{\lambda_2}{\lambda_3}$[f]	Class[g]
D1	18.97 - 19.02	-0.76	19.9	13.3	16.3	TD
D2	22.96 - 22.97	-19.6	20.0	0.43	10.1	RD
D3	23.22 - 23.223	-19.2	20.2	0.22	9.34	RD
D4	23.96 - 24.967	-18.3	19.0	0.17	30.4	RD
D5	28.33 - 28.375	-18.4	19.0	0.30	8.11	RD
D6	30.96 - 30.973	18.0	18.9	0.51	64.3	RD
D7	32.627 - 32.628	-18.5	18.9	0.32	7.01	RD
D8	37.995 - 38.015	-21.4	21.6	0.09	71.1	RD
D9	40.328 - 40.333	-19.7	21.2	0.28	5.13	RD
D10	42.57 - 42.59	28.4	30.0	0.45	5.45	RD
D11	45.567 - 45.585	16.3	21.3	0.15	3.10	RD
D12	46.455 - 46.458	22.5	24.0	0.51	7.42	RD
D13	46.464 - 46.466	23.0	24.4	0.32	7.17	RD
D14	46.474 - 46.475	24.0	24.4	0.16	13.0	RD
D15	46.881 - 46.882	24.4	24.8	0.14	88.4	RD
D16	46.896 - 46.897	24.3	24.7	0.14	13.7	RD

[a]Index number of discontinuities studied in this paper as identified in Figure 1.
[b]Time interval of discontinuity in sequential hours from 0000 UT October 18.
[c]Average B_n for the interval.
[d]Larger of the field magnitudes on either side of the discontinuity.
[e]Difference in the total field across a discontinuity.
[f]Ratio of intermediate to minimum eigenvalues.
[g]Classification of discontinuity: RD is rotational, and TD is tangential.

min of data in the same format as Figure 3. Minimum variance analysis (Table 2) yields $(\lambda_2/\lambda_3) = 64.3$, with $B_n = 18.0$ nT. The quantity $B_n/|\mathbf{B}|$ for this DD is 0.95 and $\|[\mathbf{B}]\|/|\mathbf{B}|$ is found to be 0.03. For this case, the minimum variance normal is (-0.38 , 0.64 , 0.67), i.e., it lies mostly in the (y-z) plane. We present the results of the field and flow tests in a different but equivalent way in Figure 5b, because this representation will be very familiar from studies of the terrestrial dayside magnetopause [Sonnerup et al., 1981]. We take a reference value by fixing the average values before the DD and subtract these from the corresponding field and flow components as we progress through the discontinuity. We then compare observed velocity vector differences with the theoretical ones as predicted by (2). For perfect agreement, the experimental differences normalized to the theoretical differences thus obtained would lie along the horizontal line. As can be see, the comparison is satisfactory: in magnitude, all the ratios agree with theoretical expectations to better than 50%, sometimes much better; in direction, the vectors all lie within a 20° angle of the horizontal line. This is a level of agreement at least comparable with results from magnetopause studies [Phan et al., 1996].

Figure 5a shows a depression in the bulk flow of ~60 km s⁻¹. Bulk flow speed decreases in RDs have been discussed by Scudder [1984], who pointed out that plasma flow enhancements ("jetting") are not a necessary condition for an RD since (2) is a vector equation.

Figure 5a shows that across the DD the proton temperature increases ~12%, and inside the discontinuity there is a systematic temperature decrease towards the "center" of the discontinuity. Furthermore, the field hodogram in the maximum variance plane departs from ideal behavior in that it is not clearly a circular arc. Again, we suggest that this is evidence of further structure, in this case, an expansion fan.

2.4. Summary of Results

The entries in Table 2 summarize the results of tests based on (1). The columns of Table 2 show from left to right, identification number of the DDs, starting with the front boundary (D1); B_n, the component of the magnetic field normal to the discontinuity; $|\mathbf{B}|$, the maximum of the field strengths on the two sides of the DD; $\|[\mathbf{B}]\|$, the difference of the field strengths across the discontinuity; the ratio of the intermediate to minimum eigenvalues; and, finally, the classification we arrive at.

In agreement with Lepping et al. [1997], we found the front boundary to be a clear TD. As for the other DDs, all normals are very well determined and the field component along the normal is large. With typical values of $B_n/B = 0.9$ and $\|[\mathbf{B}]\|/B = 0.02$, tests based on (1) are easily satisfied, and we conclude that all other DDs are RD's.

The results based on (2) and (3) were generally inconclusive. Some results agreed with the field analysis, whereas others did not.

Examining the changes in the density and proton temperatures across the DDs, we find in general jumps in the temperature but none in the density. We recall that the density is at lower resolution than the temper-
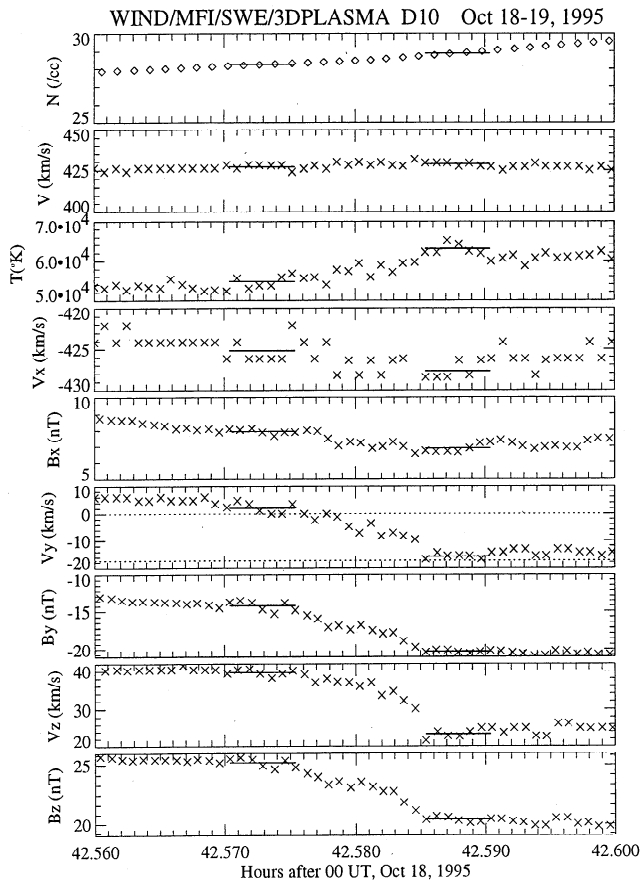
Figure 4. Wind magnetic field and plasma data at 3-s resolution for the discontinuity centered at 42.58 hours (18.58 UT, October 19, 1995). The solid lines are the average values before and after each discontinuity. Across the discontinuity there is no flow enhancement, the density is constant, but the temperature increases.
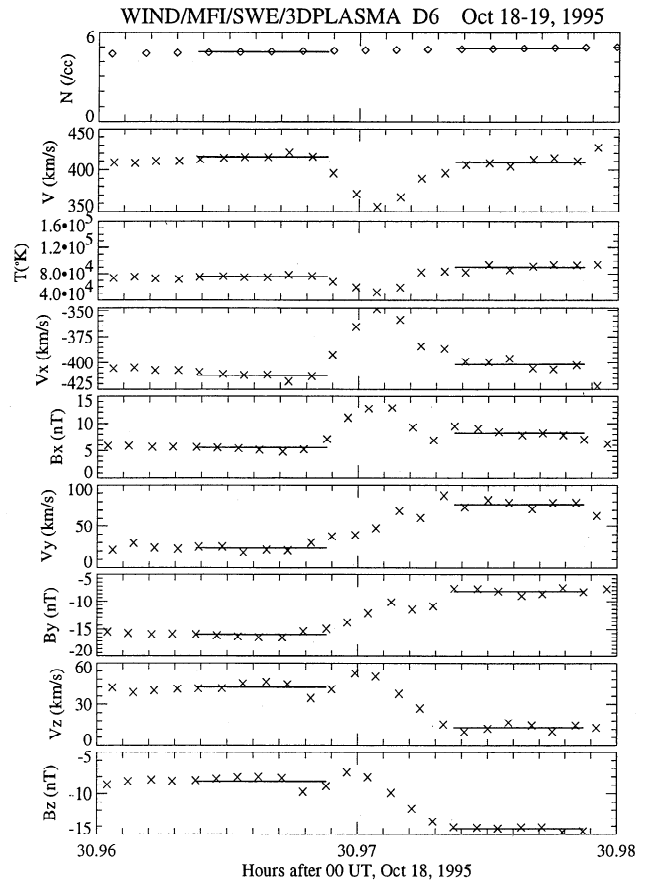
Figure 5a. Wind magnetic field and plasma data at 3-s resolution for the discontinuity centered at 30.97 UT, hours (6.97 UT, October 19, 1995). In this case, the flow speed decreases, the proton temperature is depressed, and the density stays constant.

ature. In view of the fact that temperature isotropy is well satisfied, the changes in the temperature is an indication of more elaborate structure than just an RD.

3. Large-Scale Perturbations

We now look for large scale disturbances, inquiring about the coherence of the magnetic cloud observed by Wind in October 1995. To this end, we form normals to contiguous hour segments of data. As soon as a given normal deviates from the preceding by a prescribed "tolerance" angle, we say that the coherency is no longer present. We then repeat the procedure and look for further, coherent structures. We set the tolerance angle at the reasonable, but quite arbitrary, value of 22°. Table 3 summarizes the results of this exercise. The columns from left to right indicate the universal time of the hour stretches, the angle between successive normals, the normal vector to a given hour segment in GSE coordinates, the ratio λ_2/λ_3 (a measure of how reliable the normal is (see above)), and a parameter ψ giving the angle between the normal to a given hour data stretch
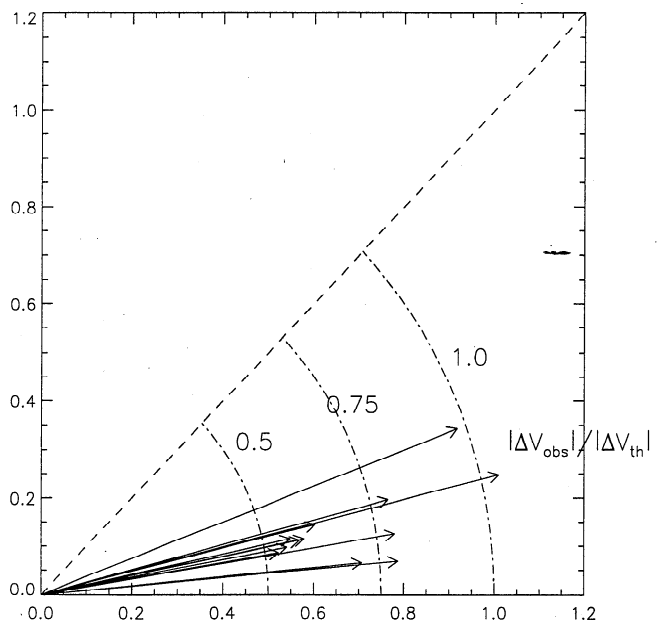

Figure 5b. Comparison of experimental results with theoretical expectations for the discontinuity shown in Figure 5a. For further details, see text.

Table 3. Minimum Variance Analysis on Successive 1-Hour Segment Intervals

Hour Intervals[a]	δ[b]	Normal Vector[c]	$\frac{\lambda_2}{\lambda_3}$[d]	ψ[e]
		Segment 1		
19.1- 20		(0.01,-0.13, 0.99)	23.2	21
20-21	11.4	(0.14, 0.02, 0.99)	6.8	21.4
21-22	10.2	(0.06, -0.14, 0.99)	40.3	23.2
22-23	21.3	(-0.28, 0.001, 0.96)	3.0	10.6
23-24	6.7	(-0.16, 0.038, 0.91)	11.7	7.5
24-25	21.3	(-0.36, 0.34, 0.87)	69.5	14.6
25-26	8.9	(-0.21, 0.37, 0.90)	46.2	12.2
26-27	5.4	(-0.29, 0.32, 0.90)	37.3	10.8
27-28	8.6	(-0.38, 0.42, 0.83)	118.	19.4
28-29	6.3	(-0.42, 0.32, 0.85)	10.2	16.8
		Segment 2		
29-30		(-0.41, 0.65, 0.64)	52.9	5.95
30-31	8.8	(-0.29, 0.62, 0.73)	21.7	5.04
31-32	4.4	(-0.22, 0.61, 0.76)	5.3	8.47
32-33	11.4	(-0.37, 0.66, 0.64)	3.9	3.70
33-34	12.1	(-0.27, 0.81, 0.53)	4.2	11.2
		Segment 3		
35-36		(-0.20, 0.98, -0.03)	6.5	13.5
36-37	4.1	(-0.25, 0.97, -0.02)	40.0	13.2
37-38	7.2	(-0.21, 0.97, -0.14)	16.4	7.68
38-39	7.3	(-0.29, 0.93, -0.23)	10.4	0.89
39-40	17.7	(-0.48, 0.77, -0.41)	7.6	17.4
40-41	18.2	(-0.22, 0.78, -0.59)	3.2	22.0

[a]Hour intervals.
[b]The δ is the angle between the normals to successive intervals.
[c]Normal vector for each interval.
[d]The λ_2/λ_3 is the ratio of intermediate to minimum eigenvalues obtained from minimum variance analysis.
[e]The ψ is the angle between the average segment normal and the normals of each hour interval comprising the segment.

and the average normal to the coherent structure to which the hour-long data stretch belongs.

With the above procedure, we find three coherent structures and a 6-hour-long stretch of data at the trailing edge of the cloud where no coherency was discernible because the normals to hour segments there could not be reliably determined. The first coherent structure stretches from cloud onset at 19.1 hours to hour 29. The normals are well determined, and the largest angle between contiguous normals does not exceed 21.3°. The totality of these normals lies inside a cone of half angle ~23°. The second coherent structure is between hours 29 and 34 (Table 3). Similar comments apply as for segment one except that the cone of normals is

even narrower, just ~11°. After a break from hour 34 to 35 (1000-1100 UT, October 19), where the normal deviates considerably from both preceding and following hour segments, a further coherent structure is found between hours 35 and 41, inclusive.

The average normals to each of the three coherent segments labeled n_1, n_2, and n_3 are listed in Table 4. The last column in this Table gives the angle γ_{ij} between the normals to segment i and segment j (i, j = 1, 2, 3). These angles are $\gamma_{12} = 35°$, $\gamma_{23} = 58°$, and $\gamma_{13} = 91°$. For comparison purposes, the field data for each of these segments are shown plotted in minimum variance coordinates in Figure 6. The format for each is as follows: from top to bottom, the total field, the

Table 4. Coherent Structures in October 18-20 Cloud

Time, UT[a]	Normal[b]	Designation	γ[d]
19.1 - 29	(-0.19, 0.16, 0.92)	n_1	$\gamma_{12} = 35°$
29 - 34	(-0.31, 0.67, 0.66)	n_2	$\gamma_{23} = 58°$
34 - 41	(-0.28, 0.90, -0.24)	n_3	$\gamma_{13} = 91°$

[a]Time intervals for the three coherent structures.
[b]Normal vector is the average normal for each segment.
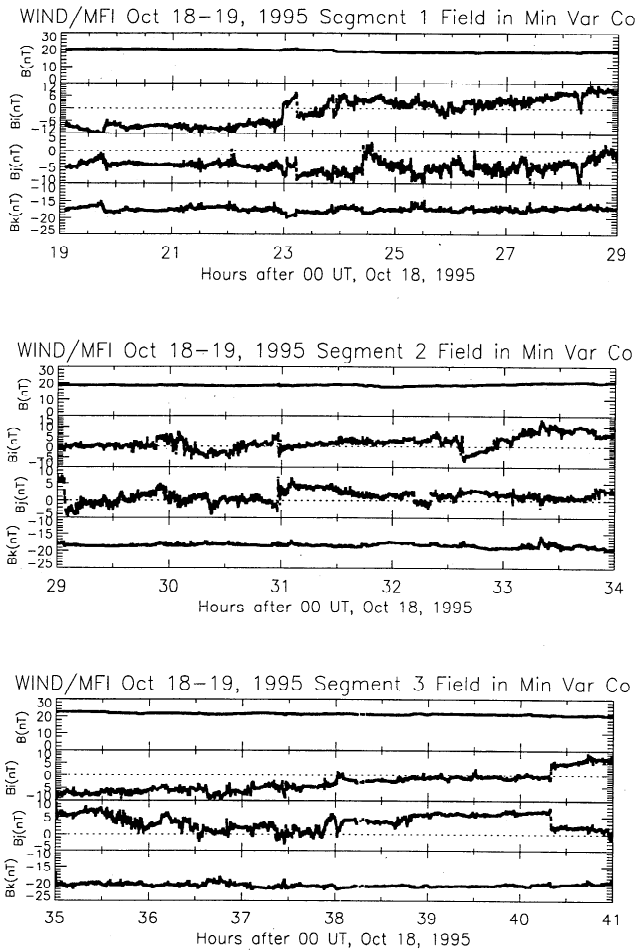[d]The γ is the angle between the normals to the segments.

Figure 6. Magnetic field in principal axes coordinates for each of the three several-hour-long segments discussed in the text.

4. Discussion and Conclusions

We have studied high-resolution magnetic field and plasma data for the October 18-19, 1995, magnetic cloud. We took as a starting point the observation that the rotation of the field was not smooth, and identified a number of directional discontinuities, restricting ourselves to a subset of these where the rotation was larger than 15° in ~1 min. Using traditional methods to examine their nature, we found that those within the magnetic cloud were all rotational discontinuities, whereas the front boundary, despite a ~100° field rotation, is a clear tangential discontinuity. These conclusions were based mainly on the magnetic field data, particularly the large nonzero field component normal to the discontinuities. This result was supported in some, but not all, cases by further tests using combined magnetic field and plasma data. There were in general temperature jumps across the DDs indicative of further structure.

We also looked at large-scale perturbations. We suggested a way of searching for coherent substructures, based on minimum variance analysis. We found evidence for both structure and lack of it. The evidence for structure consisted of three several-hour-long segments of data where (1) each segment has a well-defined normal; and (2) the normals to the segments are oriented differently with respect to each other. Furthermore, we obtain a substantially different normal if we carry out a minimum variance analysis on the totality of cloud data. We found no evidence of structure in the last 6 hours of cloud passage, and for 1 hour (1000-1100 UT,
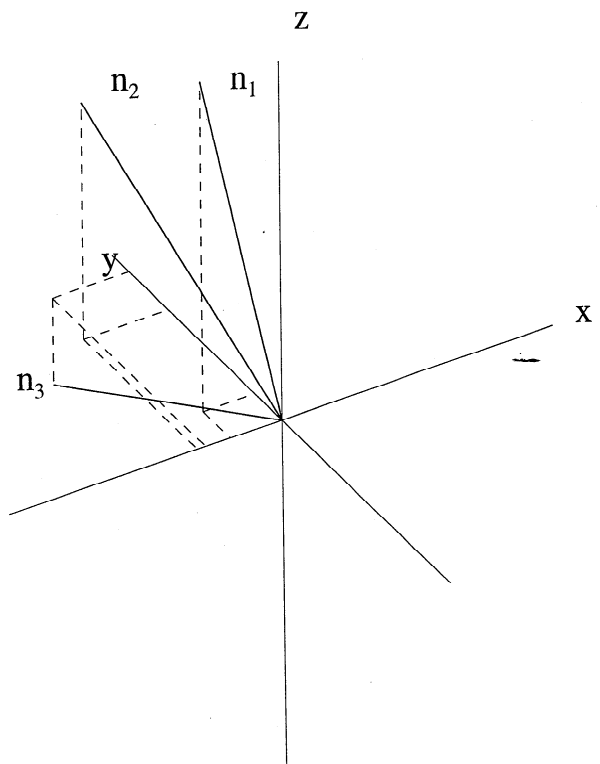
field components in the maximum variance plane, and, finally, the field component in the minimum variance direction. Clearly, despite the three very different normals, the data plotted in the respective principal axes coordinates are in all three cases very satisfactory. The orientation of these normals in a GSE coordinate system is shown in Figure 7. If we were to carry out a minimum variance analysis on the data for the entire ~29 hours of the cloud interval in Figure 1, we would get a normal of (0.96, 0.29, 0.00) with $\lambda_2/\lambda_3 = 5.6$, i.e., very different from the the normals to each of the three coherent segments. In summary, we may say that there is clear substructure in, and/or distortion of, in the October 1995 cloud.

Finally, we inquire about the relationship between the DDs (what we may call the fine structure) and the coherent segments (what we may, in turn, call the large scale structure). Forming the angle between the DD normals and the average normal to the segment where a given DD occurs, we find that all DD normals are closely aligned with the segment normal, the largest deviation being ~20° and occurring in segment 1.

Figure 7. Orientation of the normals for the three coherent segments in a GSE coordinate system.

October 19) between segments 2 and 3. The normals to the RDs within a given segment are closely aligned to the normal to that segment.

Our finding of rotational discontinuities within the cloud allows for the possibility of reconnection, perhaps between the adjacent bundles of field lines within the cloud. This latter scenario was investigated by *Larson et al.* [1997]. Examining the same cloud with the use of heat flux electrons (in the energy range ~ 0.1 − 1 keV) and energetic (1-100 keV) electrons, Larson et al. concluded that there were three types of field line topologies present inside the cloud: some field lines were connected at both ends to the Sun, some were connected only at one end, and some others were completely disconnected from the Sun [see *Larson et al.*, 1997, Figure 3]. Larson et al. attributed the disconnections to reconnection of cloud magnetic field lines with themselves. Though not the detail, our results complement the general conclusions of Larson et al.'s work. For example, at the rear of the cloud, these authors find repeated disconnections (see their Figure 1), and we, in turn, fail to find evidence of structure there, as defined above, but we find instead many RDs. A similar correspondence occurs at 0700 and 1000 UT, October 19 (hours 31 and 34, respectively). Prior to 0700 UT, electron heat fluxes of energies 118 and 290 eV, respectively, are bidirectionally streaming along the magnetic field. At 0700 UT this is interrupted, and becomes unidirectional. At 1000 UT, there is a complete dropout in both energy channels [see *Larson et al.*, 1997, panels I and J]. In our case, we find the presence of a RD (DD6) at ~0700 UT, and at 1000 UT we infer a clear break in a coherent structure.

The substructures that we found appear to be misaligned with respect to each other because the normals, which we believe to be very well determined, point in substantially different directions. In addition, these normals are not along the minimum variance normal of the whole configuration, which is mainly along the GSE x direction. In line with minimum variance analyses of cloud data in the past, we obtain a small normal component for the whole configuration, whereas we obtain a large normal component for each substructure. It could be that the interaction with the ambient medium contributed in part to what appear to us as substructures by, for example, grossly distorting the flux tube. As noted earlier, the cloud is running into dense material ahead, and is being overtaken by faster material from behind. However, the agreement we found between interruptions in the flow properties of electrons, on the one hand, and interruptions of structure, on the other, suggests that the interaction with the medium alone is not the full explanation.

The Editor thanks J. E. Sorensen and R. Goldstein for their assistance in evaluating this paper.

References

Acuna, M. H., et al., The global Geospace Science Program and its investigations, *Space Sci. Rev., 71*, 5, 1995.

Belcher, J. W., and C. V. Solodnya, Alfven waves and directional discontinuities in the interplanetary medium, *J. Geophys. Res., 80*, 181, 1975.

Burlaga, L. F., Directional discontinuities in the interplanetary magnetic field, *Sol. Phys., 7*, 54, 1969.

Burlaga, L. F., Nature and origin of directional discontinuities in the solar wind, *J. Geophys. Res., 76*, 4360, 1971.

Burlaga, L. F., *Interplanetary Magnetohydrodynamics*, 329 pp., Oxford Univ. Press, New York, 1995.

Burlaga, L. F., E. Sittler Jr., F. Mariani, and R. Schwenn, Magnetic loop behind an interplanetary shock: Voyager, Helios and IMP 8 observations, *J. Geophys. Res., 86*, 6673, 1981.

Burlaga, L. F., R. P. Lepping, and J. Jones, Global configuration of a magnetic cloud, in *Physics of Magnetic Flux Ropes, Geophys. Monogr. Ser.*, vol. 58, edited by C. T. Russell, E. R. Priest, and L. C. Lee, p. 373, AGU, Washington, D. C., 1990.

Burlaga, L. F., et al., A magnetic cloud observed by Wind on October 18 - 20, 1995, internal document, Lab. for Extraterrestrial Phys., NASA Goddard Space Flight Cent., Greenbelt, Md., Feb. 1996.

Burlaga, L. F., et al., A magnetic cloud containing prominence material: January 1997, *J. Geophys. Res., 103*, 277, 1998.

Farrugia, C. J., L. F. Burlaga, V. A. Osherovich, and R. P. Lepping, A comparative study of dynamically expanding force-free, constant-alpha magnetic configurations with applications to magnetic clouds, *Solar Wind Seven*, edited by E. Marsch and R. Schwenn, p. 611, Pergamon, New York, 1992.

Farrugia, C. J., L. F. Burlaga, V. A. Osherovich, I. G. Richardson, M. P. Freeman, R. P. Lepping, and A. Lazarus, A study of an expanding interplanetary magnetic cloud and its interaction with the Earth's magnetosphere: The interplanetary aspect, *J. Geophys. Res., 98*, 7621, 1993.

Gosling, J. T., D. N. Baker, S. J. Bame, W. C. Feldman, R. D. Zwickl, and E. J. Smith, Bidirectional solar wind electron heat flux events, *J. Geophys. Res., 92*, 8519, 1987.

Hudson, P. D., Discontinuities in an anisotropic plasma and their identification in the solar wind, *Planet. Space Sci., 18*, 1161, 1970.

Larson, D. E., et al., Tracing the topology of the October 18-20, 1995, magnetic cloud with ~0.1 - 10^2 keV electrons, *Geophys. Res. Lett., 24*, 1911, 1997.

Lepping, R. P., et al., The WIND magnetic field investigation, *Space Sci. Rev., 71*, 207-229, 1995.

Lepping, R. P., et al., The WIND magnetic cloud and events of October 18-20, 1995: Interplanetary properties and as triggers for geomagnetic activity, *J. Geophys. Res., 102*, 14,049, 1997.

Lepping, R. P., and K. W. Behannon, Magnetic field directional discontinuities, 1, Minimum variance errors, *J. Geophys. Res., 85*, 4695, 1980.

Lin, R. P., et al., A three-dimensional plasma and energetic particle investigation for the Wind spacecraft, *Space Sci. Rev., 71*, 125-153, 1995.

Neugebauer, M, D. R. Clay, B. E. Goldstein, B. T. Tsurutani, and R. D. Zwickl, A reexamination of rotational and tangential discontinuities in the solar wind, *J. Geophys. Res., 89*, 5395, 1984.

Ogilvie, K. W., et al., SWE, A comprehensive plasma instrument for the WIND spacecraft, *Space Sci. Rev., 71*, 55-77, 1995.

Osherovich, V. A., C. J. Farrugia, and L. F. Burlaga, Dynamics of aging magnetic clouds, *Adv. Space Res., 13(6)*, 57, 1993.

Parks, G. K., *Physics of Space Plasmas: An Introduction*, Addison Wesley, Reading, Mass., 1991.

Phan, T.-D., G. Paschmann, and B. U. O. Sonnerup, Low-latitude dayside magnetopause and boundary layer for high magnetic shear, 2, Occurrence of magnetic reconnection, *J. Geophys. Res., 101*, 7817, 1996.

Scudder, J. D., Fluid signatures of rotational discontinuities at the Earth's magnetopause, *J. Geophys. Res., 89*, 7431, 1984.

Sonnerup, B. U. O., and L. J. Cahill, Magnetopause structure and attitude from Explorer 12 observations, *J. Geophys. Res., 72*, 171, 1967.

Sonnerup, B. U. O., G. Paschmann, I. Papamastorakis, N. Sckopke, G. Haerendel, S. J. Bame, J. R. Asbridge, J. T. Gosling, and C. T. Russell, Evidence for magnetic field reconnection at the Earth's magnetopause, *J. Geophys. Res., 86*, 10,049, 1981.

C. J. Farrugia, L. Janoo, J. M. Quinn, and R. B. Torbert, Institute for the Study of Earth, Oceans, and Space, University of New Hampshire, Durham, NH 03824. (e-mail: lxj@cs.unh.edu, farrugia@monet.sr.unh.edu, jack.quinn@unh.edu, roy.torbert@unh.edu)

D. Larson and R. P. Lin, Space Sciences Laboratory, University of California, Berkeley, CA 94720.

R. P. Lepping, K. W. Ogilvie, and A. Szabo, NASA Goddard Space Flight Center, Code 692, Greenbelt, MD 20771.

V. A. Osherovich, NASA Goddard Space Flight Center, Hughes STX, Greenbelt, MD 20771.

J. D. Scudder, Department of Physics and Astronomy, University of Iowa, Iowa City, IA 52240.

J. T. Steinberg, Center for Space Research, Massachusetts Institute of Technology, Cambridge, MA 02139.